Research Article | Vol. 25, No. 9 | 1 May 2017 | OPTICS EXPRESS 9734

Optics EXPRESS

Stable angular emission spectra in white organic light-emitting diodes using graphene/PEDOT:PSS composite electrode

HYUNSU CHO,[1] HYUNKOO LEE,[1] JONGHEE LEE,[1] WOO JIN SUNG,[1] BYOUNG-HWA KWON,[1] CHUL-WOONG JOO,[1] JIN-WOOK SHIN,[1] JUN-HAN HAN,[1] JAEHYUN MOON,[1] JEONG-IK LEE,[1] SEUNGMIN CHO,[2] AND NAM SUNG CHO[1,*]

[1]*ICT Materials & Components Research Laboratory, Electronics and Telecommunications Research Institute (ETRI), 218 Gajeong-ro, Yuseong-gu, Daejeon, South Korea*
[2]*Hanwha Techwin R&D Center, 6 Pangyo-ro 319 beon-gil, Bundang-gu, Seongnam-si, Gyeonggi-do, South Korea*
**kevinchons@etri.re.kr*

Abstract: In this work, we suggest a graphene/ poly (3,4-ethylenedioxythiophene) polystyrene sulfonate (PEDOT:PSS) composite as a transparent electrode for stabilizing white emission of organic light-emitting diodes (OLEDs). Graphene/PEDOT:PSS composite electrodes have increased reflectance when compared to graphene itself, but their reflectance is still lower than that of ITO itself. Changes in the reflectance of the composite electrode have the advantage of suppressing the angular spectral distortion of white emission OLEDs and achieving an efficiency of 16.6% for white OLEDs, comparable to that achieved by graphene-only electrodes. By controlling the OLED structure to compensate for the two-beam interference effect, the CIE color coordinate change (Δxy) of OLEDs based on graphene/PEDOT:PSS composite electrodes is 0.018, less than that based on graphene-only electrode, i.e.,0.027.

OCIS codes: (230.0230) Optical devices; (230.3670) Light-emitting diodes.

References and links

1. K. S. Kim, Y. Zhao, H. Jang, S. Y. Lee, J. M. Kim, K. S. Kim, J.-H. Ahn, P. Kim, J.-Y. Choi, and B. H. Hong, "Large-scale pattern growth of graphene films for stretchable transparent electrodes," Nature **457**(7230), 706–710 (2009).
2. S. Pang, Y. Hernandez, X. Feng, and K. Müllen, "Graphene as transparent electrode material for organic electronics," Adv. Mater. **23**(25), 2779–2795 (2011).
3. T.-H. Han, S.-H. Jeong, Y. Lee, H.-K. Seo, S.-J. Kwon, M.-H. Park, and T.-W. Lee, "Flexible transparent electrodes for organic light-emitting diodes," J. Inf. Disp. **16**(2), 71–84 (2015).
4. V. G. Kravets, A. N. Grigorenko, R. R. Nair, P. Blake, S. Anissimova, K. S. Novoselov, and A. K. Geim, "Spectroscopic ellipsometry of graphene and an exciton-shifted van Hove peak in absorption," Phys. Rev. B **81**(15), 155413 (2010).
5. S.-Y. Kim and J.-J. Kim, "Outcoupling efficiency of organic light emitting diodes employing graphene as the anode," Org. Electron. **13**(6), 1081–1085 (2012).
6. H. Cho, J.-W. Shin, N. S. Cho, J. Moon, J.-H. Han, Y.-D. Kwon, S. Cho, and J.-I. Lee, "Optical effects of graphene electrodes on organic light-emitting diodes," IEEE J. Sel. Top. Quantum Electron. **22**(1), 2000206 (2016).
7. T.-H. Han, Y. Lee, M.-R. Choi, S.-H. Woo, S.-H. Bae, B. H. Hong, J.-H. Ahn, and T.-W. Lee, "Extremely efficient flexible organic light-emitting diodes with modified graphene anode," Nat. Photonics **6**(2), 105–110 (2012).
8. N. Li, S. Oida, G. S. Tulevski, S.-J. Han, J. B. Hannon, D. K. Sadana, and T.-C. Chen, "Efficient and bright organic light-emitting diodes on single-layer graphene electrodes," Nat. Commun. **4**, 2294 (2013).
9. J. Hwang, H. K. Choi, J. Moon, T. Y. Kim, J.-W. Shin, C. W. Joo, J.-H. Han, D.-H. Cho, J. W. Huh, S.-Y. Choi, J.-I. Lee, and H. Y. Chu, "Multilayered graphene anode for blue phosphorescent organic light emitting diodes," Appl. Phys. Lett. **100**(13), 133304 (2012).

#286460 https://doi.org/10.1364/OE.25.009734
Journal © 2017 Received 9 Feb 2017; revised 29 Mar 2017; accepted 16 Apr 2017; published 19 Apr 2017

Optics EXPRESS

10. J. Tae Lim, H. Lee, H. Cho, B.-H. Kwon, N. Sung Cho, B. Kuk Lee, J. Park, J. Kim, J.-H. Han, J.-H. Yang, B.-G. Yu, C.-S. Hwang, S. Chu Lim, and J.-I. Lee, "Flexion bonding transfer of multilayered graphene as a top electrode in transparent organic light-emitting diodes," Sci. Rep. **5**, 17748 (2015).
11. J. Lee, T.-H. Han, M.-H. Park, D. Y. Jung, J. Seo, H.-K. Seo, H. Cho, E. Kim, J. Chung, S.-Y. Choi, T.-S. Kim, T.-W. Lee, and S. Yoo, "Synergetic electrode architecture for efficient graphene-based flexible organic light-emitting diodes," Nat. Commun. **7**, 11791 (2016).
12. E. C.-W. Ou, L. Hu, G. C. R. Raymond, O. K. Soo, J. Pan, Z. Zheng, Y. Park, D. Hecht, G. Irvin, P. Drzaic, and G. Gruner, "Surface-modified nanotube anodes for high performance organic light-emitting diode," ACS Nano **3**(8), 2258–2264 (2009).
13. C.-H. Song, K.-H. Ok, C.-J. Lee, Y. Kim, M.-G. Kwak, C. J. Han, N. Kim, B.-K. Ju, and J.-W. Kim, "Intense-pulsed-light irradiation of Ag nanowire-based transparent electrodes for use in flexible organic light emitting diodes," Org. Electron. **17**, 208–215 (2015).
14. Y.-S. Liu, J. Feng, X.-L. Ou, H. Cui, M. Xu, and H.-B. Sun, "Ultrasmooth, highly conductive and transparent PEDOT:PSS/silver nanowire composite electrode for flexible organic light-emitting devices," Org. Electron. **31**, 247–252 (2016).
15. Y.-H. Huang, W.-L. Tsai, W.-K. Lee, M. Jiao, C.-Y. Lu, C.-Y. Lin, C.-Y. Chen, and C.-C. Wu, "Unlocking the full potential of conducting polymers for high-efficiency organic light-emitting devices," Adv. Mater. **27**(5), 929–934 (2015).
16. J. Ryu, Y. Kim, D. Won, N. Kim, J. S. Park, E.-K. Lee, D. Cho, S.-P. Cho, S. J. Kim, G. H. Ryu, H.-A.-S. Shin, Z. Lee, B. H. Hong, and S. Cho, "Fast synthesis of high-performance graphene films by hydrogen-free rapid thermal chemical vapor deposition," ACS Nano **8**(1), 950–956 (2014).
17. S. J. Kim, J. Ryu, S. Son, J. M. Yoo, J. B. Park, D. Won, E.-K. Lee, S.-P. Cho, S. Bae, S. Cho, and B. H. Hong, "Simultaneous etching and doping by cu-stabilizing agent for high-performance graphene-based transparent electrodes," Chem. Mater. **26**(7), 2332–2336 (2014).
18. H. A. Macleod, *Thin-film Optical Filters* (Taylor & Francis, 2001)
19. H. Moon, H. Cho, M. Kim, K. Takimiya, and S. Yoo, "Towards colorless transparent organic transistors: potential of benzothieno[3,2-b]benzothiophene-based wide-gap semiconductors," Adv. Mater. **26**(19), 3105–3110 (2014).
20. S. Albrecht, S. Schäfer, I. Lange, S. Yilmaz, I. Dumsch, S. Allard, U. Scherf, A. Hertwig, and D. Neher, "Light management in PCPDTBT:PC70BM Solar Cells: a comparison of standard and inverted device structures," Org. Electron. **13**(4), 615–622 (2012).
21. H. Cho, C. Yun, and S. Yoo, "Multilayer transparent electrode for organic light-emitting diodes: tuning its optical characteristics," Opt. Express **18**(4), 3404–3414 (2010).
22. J.-H. Kim, J. Seo, D.-G. Kwon, J.-A. Hong, J. Hwang, H. K. Choi, J. Moon, J.-I. Lee, D. Y. Jung, S.-Y. Choi, and Y. Park, "Carrier injection efficiencies and energy level alignments of multilayer graphene anodes for organic light-emitting diodes with different hole injection layers," Carbon **79**, 623–630 (2014).
23. H.-W. Lin, W.-C. Lin, J.-H. Chang, and C.-I. Wu, "Solution-processed hexaazatriphenylene hexacarbonitrile as a universal hole-injection layer for organic light-emitting diodes," Org. Electron. **14**(4), 1204–1210 (2013).
24. E. Najafabadi, K. A. Knauer, W. Haske, and B. Kippelen, "High-performance inverted top-emitting green electrophosphorescent organic light-emitting diodes with a modified top Ag anode," Org. Electron. **14**(5), 1271–1275 (2013).
25. H. Lee, J. Lee, S. Park, Y. Yi, S. W. Cho, J. W. Kim, and S. J. Kang, "Hole injection enhancement of a single-walled carbon nanotube anode using an organic charge-generation layer," Carbon **71**, 268–275 (2014).

1. Introduction

As a material for transparent electrodes in optoelectronic devices, graphene has superior flexibility and transmittance characteristics [1–3]. Despite posing issues for scalability and physical/chemical stability and presenting a trade-off between transmittance and sheet resistance, graphene is still regarded as a promising material for transparent electrodes. The distinguishing characteristics of graphene are that it is both ultrathin and conductive. The single-layer thickness of graphene is only 0.34 nm with a sheet resistance on the order of a few hundred ohms per square. Though its refractive index is ~1-2 and its extinction coefficient is larger than 2, it ultrathin property results in high transmittance [4].

When graphene is applied to transparent electrodes in organic light-emitting diodes (OLEDs), the above characteristics result in unique optical properties when compared to OLEDs based on indium tin oxide (ITO) electrodes. Due to stack structure and thickness, the optical cavity effect is intrinsically present in OLEDs. The presence of this cavity effect mainly results from the reflectance of electrode surfaces and the refractive contrast of the organics/electrode interface. Because the reflectance of graphene is lower than that of the more conventionally used ITO material, the cavity effect is greatly reduced in OLEDs with graphene-based electrodes [5,6]. Thus, optically optimized ITO-based OLEDs always yield

Optics EXPRESS

higher efficiencies than graphene-based OLEDs. Nevertheless, it is notable that graphene-based OLEDs have exhibited efficiencies comparable to those achieved by ITO-based OLEDs though the number of graphene layers strongly influences OLED efficiency [7–10]. Additionally, graphene has been utilized in multilayer electrodes, sandwiched between high-index and low-index layers instead of thin metal layers; this results in enhanced cavity resonance in OLED devices and has yielded higher efficiencies than in thin metal-based electrodes [11].

In OLEDs based on graphene electrodes, a poly (3,4-ethylenedioxythiophene) polystyrene sulfonate (PEDOT:PSS) layer (or a derivative thereof) has frequently been used as a hole injection material [7, 8]. From a structural view point, the solution processed PEDOT:PSS layer covers protruding parts of the graphene and yields a surface with low roughness, leading to electrically stable device operation. As a result, it has been also widely used not only in graphene electrodes but also in electrodes using ITO, Ag nanowire, and other alternatives [12–14]. Moreover, studies have shown the possibility of modulating the optical properties of ITO with the addition of a PEDOT:PSS layer [15]. The refractive index of PEDOT:PSS (n ~1.5), is lower than that of typical organic layers and of ITO (n ~1.8), resulting in index contrast within the OLED structure, i.e. glass (n ~1.5, low-index)/ITO (high-index)/PEDOT:PSS (low-index)/organic layers (high-index). As a result, due to the formation of a sharp optical interface between the PEDOT:PSS and ITO layers, an anode structure of ITO/PEDOT:PSS can induce a microcavity effect in the OLED. With carefully adjusted device thickness, the OLED with the ITO/PEDOT:PSS electrode is expected to have a much higher efficiency than that with the ITO electrode.

In this study, we investigate the optical effect of a PEDOT:PSS layer in graphene-based white OLEDs in order to analyze optical properties in a wide wavelength region. White OLEDs based on graphene electrodes have been studied, but these studies focused on demonstrating their efficiency [7, 8]. In white OLEDs, color qualities such as color coordinates and color shift for viewing angles are as important as efficiency. Although a PEDOT:PSS layer is primarily applied in graphene-based OLEDs for electrical stability, it is also required to study optical effects of PEDOT:PSS in graphene/PEDOT:PSS composite electrodes as in ITO/PEDOT:PSS electrodes. Here, the change in angular emission spectra of white OLEDs was focused to account for the presence of a PEDOT:PSS layer on graphene electrodes.

2. Experiments

A 70-nm-thick ITO-deposited glass was prepared as a reference electrode. Single-layer graphene film obtained using a chemical vapor method on a Cu foil was transferred sequentially in order to form a 4-layered graphene anode [16, 17]. Both substrates were cleaned by ultra-sonication in acetone and isopropyl alcohol (IPA). A PEDOT:PSS (CLEVIOS P VP AI 4083, Heraeus) layer was spin-coated at 3000 rpm for 30 s on UVO-treated substrates, followed by thermal annealing on a 120°C hot plate. This process results in a PEDOT:PSS layer with a thickness of about 40 nm. The transmittances of the four kinds of substrates were measured using an UV-Vis spectrometer (LAMBDA 750, PerkinElmer). All the prepared substrates were kept in a vacuum oven before they were loaded into a thermal evaporation chamber.

Optics EXPRESS

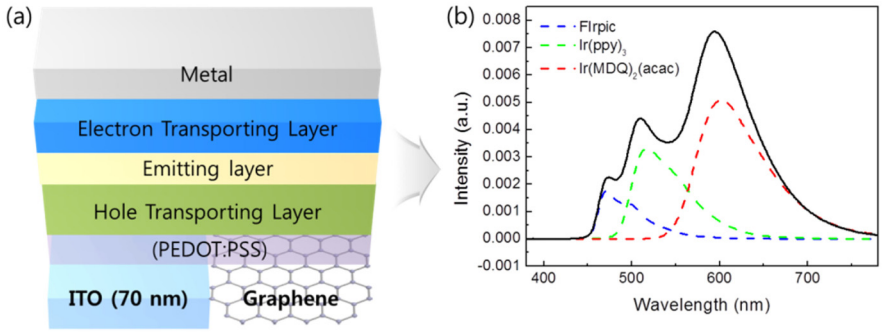

Fig. 1. (a) Schematics of OLED structures under study and (b) electroluminescent spectra of blue, green and red dopants for constructing the white spectrum.

As shown in Fig. 1(a), an OLED device consists of a hole transporting layer (HTL), an emission layer (EML), an electron transporting layer (ETL) and a LiF/Al cathode. The HTL was constructed with a 4-times combination of Dipyrazino[2,3-f:2',3'-h]quinoxaline 2,3,6,7,10,11-hexacarbonitrile (HAT-CN, 10 nm)/ N,N′-Di(1-naphthyl)-N,N′-diphenyl-(1,1′-biphenyl)-4,4′-diamine (NPB, 45 nm) and HAT-CN (10 nm)/ 4,4′-Cyclohexylidenebis[N,N-bis(4-methylphenyl)benzenamine] (TAPC, 50 nm). The white emission spectrum is combined with Bis[2-(4,6-difluorophenyl)pyridinato-C2,N](picolinato)iridium(III) (FIrpic), Tris[2-phenylpyridinato-C2,N]iridium(III) ($Ir(ppy)_3$), and Bis(2-methyldibenzo[f,h]quinoxaline) (acetylacetonate)iridium(III) ($Ir(MDQ)_2(acac)$) for blue, green and red, respectively as shown in Fig. 1(b). Tris(4-carbazoyl-9-ylphenyl)amine (TCTA) doped with FIrpic (7%, 5 nm), Ir(MDQ)2(acac) (5%, 0.5 nm), and $Ir(ppy)_3$ (7%, 1 nm), and 2,6-Bis[3-(9H-carbazol-9-yl)phenyl]pyridine (DCzPPy) doped with FIrpic (7%, 10 nm) were used as an EML. Finally, 1,3-bis(3,5-dipyrid-3-yl-phenyl)benzene (BmPyPB, 60 nm) was deposited as an ETL. A source meter (Keithley 238), a goniometer-equipped spectroradiometer (Minolta CS-2000), and an integrating sphere (HM-series, Otsuka Electronics Korea Co.) were used to measurd the electrical and optical properties of the OLEDs.

3. Results and discussion

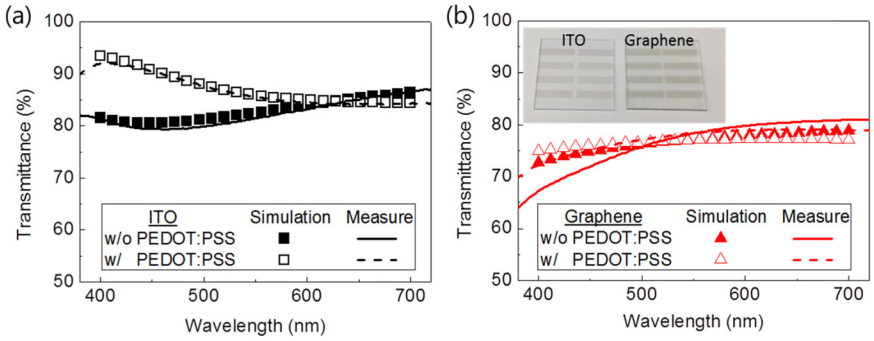

Fig. 2. Measured and simulated transmittances of the (a) ITO and (b) graphene electrodes in the presence of a PEDOT:PSS layer. Inset: images of patterned ITO and graphene electrodes.

To discuss optical phenomena in OLED structures for different transparent electrodes, their transmittance and reflectance should be considered from the incident media of the organic layer, rather than from air. Those values can be calculated by optical simulation based on the transfer matrix method [18]. Before performing simulation, an optical constant in addition to the thicknesses of ITO, graphene and PEDOT:PSS must be confirmed in order to perform reliable simulations, as the processing conditions can significantly alter the optical constants.

Optics EXPRESS

Figures 2(a) and 2(b) show the measured and calculated transmittance of the structure consisting of: air/ glass (incoherent)/ ITO or graphene / PEDOT:PSS or nothing/air. Considering that the simulation values are fitted nicely with the measured values, it is confirmed that the optical constants borrowed from the literature and the thicknesses of each material are well defined [19, 20]. By tuning the thickness of the graphene electrode, the average transmittance value can be adjusted by about 75%, but the transmittance dispersion is not well fitted. Though other optical constants of graphene were also applied for simulation, the transmittance dispersion still showed a gap between the measured and simulated data. Such a difference may originate from the doping material such as benzimidazole sandwiched between films to enhance the electrical conductivity and stability during the simultaneous etching and doping process [17].

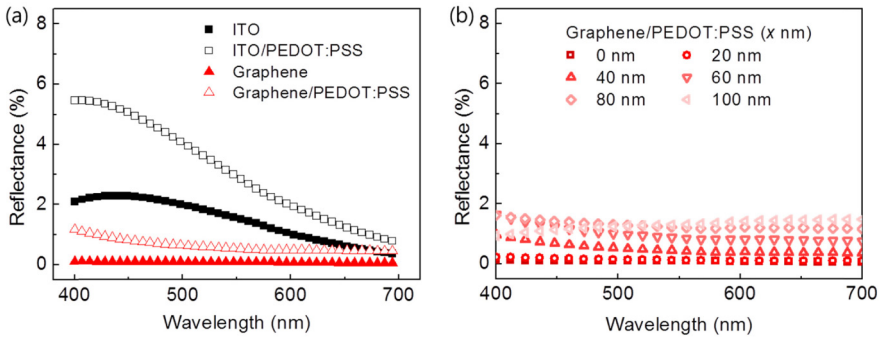

Fig. 3. (a) The calculated reflectance of the structure of TAPC/*x*/Glass with *x* being ITO, ITO/PEDOT:PSS, graphene, and graphene/PEDOT:PSS. (b) The change in the calculated reflectance of the structure of TAPC/graphene/PEDOT:PSS/Glass for PEDOT:PSS thicknesses.

Figure 3(a) shows the simulated reflectance of the structures of TAPC/ *x*/ Glass with *x* being ITO, ITO/PEDOT:PSS, graphene, and graphene/PEDOT:PSS. ITO has a higher reflectance than graphene, which may result in an enhanced cavity effect. If a PEDOT:PSS layer is applied to the each electrode, the reflectance of the composite electrodes is increased. However, the graphene/PEDOT:PSS composite electrode still has a lower reflectance than ITO-only electrode. In the case of the ITO/PEDOT:PSS composite electrode, the thickness has a significant effect on the optical properties of the OLEDs [15]. On the other hand, the reflectance of the graphene/PEDOT:PSS composite does not vary significantly. For the PEDOT:PSS thickness range of 0-100 nm, the reflectance does not exceed 2% as shown in Fig. 3(b). These simulation results show that the optical contrast at the graphene/PEDOT:PSS interface is not high enough to bring forth a noticeable change in transmittance and reflectance. Such a feature can be useful for lessening cavity effects and stabilizing the angular emission of white emission spectra.

The optical simulations on white OLED devices were performed using commercial software (SETFOS, Fluxim) based on the optical properties of the electrode materials. In order to explore the optical effects without electrical losses, we fixed the EML and ETL thicknesses at 20 nm and 60 nm, respectively, and varied the HTL thickness. A white emission spectrum for optical simulation was assumed as shown in Fig. 1(b). In accordance with these HTL thicknesses and emission angles, the emission spectra of OLEDs with ITO and graphene electrodes were simulated.

Optics EXPRESS

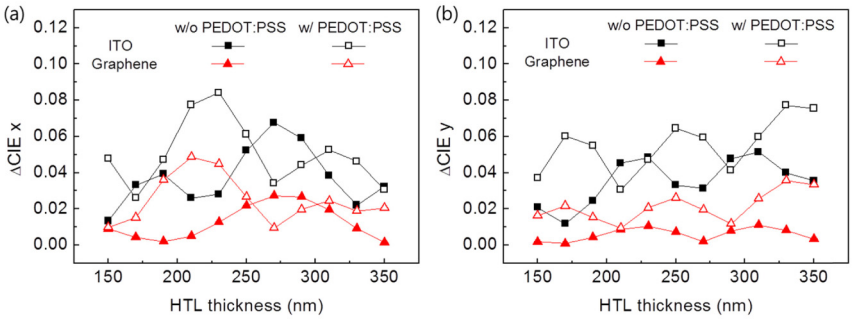

Fig. 4. CIE (a) x-coordinate and (b) y-coordinate changes for OLEDs with ITO and graphene electrodes against an emission angle range of 0° to 70° and varying HTL thicknesses.

Figures 4(a) and 4(b) show the variations in CIE *x*-coordinates and *y*-coordinates of OLEDs with ITO and graphene electrodes against an emission angle range of 0° to 70° as functions of HTL thickness. By using the optical simulation, the CIE *x*- and *y*-coordinates at different angles (0-70°) were obtained (see Data File 1) and then the largest difference between angles was calculated. The OLED using graphene shows better coordinate stability than its counterpart. The variation in CIE *x*-coordinate fluctuates as the HTL thickness changes, but remains below 0.03. Moreover, the variation in CIE *y*-coordinate remains less than ~0.01 independently of the HTL thickness. The graphene-based OLED was related to a negligible microcavity effect, resulting in marginal changes in the angular emission spectra, as reported in our previous work on monochromatic graphene anode OLEDs [6]. Such advantageous emission characteristics are similarly observed in graphene-based white OLEDs. On the other hand, in the case of the ITO electrodes, cavity enhancement for specific wavelengths causes a large spectral shift in white OLEDs for different viewing angles. The changes in CIE coordinates for the ITO-based device are larger than 0.2 despite the well-designed device structures. This effect deteriorates the quality of the white emission.

The graphene/PEDOT:PSS composite electrode induces some optical effects in spite of the ultrathin thickness of the graphene layer and the similar refractive indexes between the glass substrate and PEDOT:PSS layers. As shown in Fig. 4, the OLEDs with graphene/PEDOT:PSS composite electrodes exhibited more fluctuation in both CIE coordinates than OLEDs with only graphene. However, the graphene/PEDOT:PSS composite-based OLEDs still had similar or better color quality than the ITO-based OLEDs. Moreover, if the HTL thickness is well controlled in the range of 250 nm to 300 nm, the graphene/PEDOT:PSS composite-based devices show less variance in the CIE *x*-coordinate, and similar or slightly larger variance in the CIE *y*-coordinate. Cavity enhancement is presented as a product of the Fabry–Pérot factor and the two-beam interference factor [21]. The former is related to the reflectance of both the transparent and reflective electrodes of OLEDs and the distance between them. The latter is related to the reflectance of the reflective electrodes and the distance between the emitter position and the reflective electrode. The variables in this study (HTL thickness and the reflectance of ITO, graphene and their respective composites) influence on the only Fabry–Pérot factor. As a result, the change in color coordinates for the OLEDs with different transparent electrodes is primarily influenced by two-beam interference. The actual color change in OLEDs is determined by whether the Fabry–Pérot factor creates destructive or constructive interference with the two-beam interference factor. Consequently, graphene/PEDOT:PSS composite electrodes can achieve electrically stable (having reduced surface roughness) and optically stable (having low color change) OLEDs if the OLED structures are designed as mentioned previously.

Optics EXPRESS

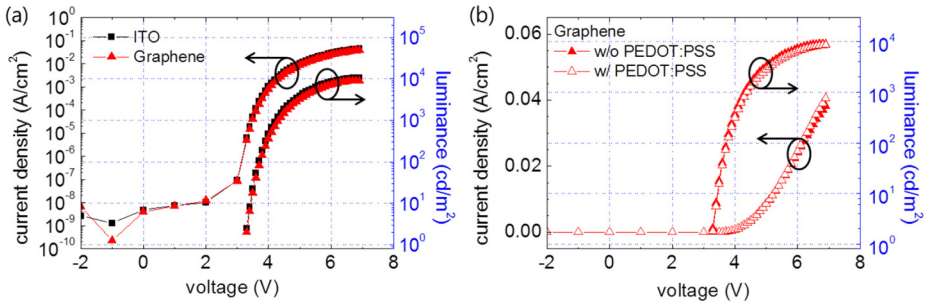

Fig. 5. Current density (*J*)-voltage (*V*)-luminance (*L*) of white OLEDs with (a) ITO and graphene electrodes and (b) graphene electrodes with and without presence of a PEDOT:PSS layer.

The basic characteristics of actual OLED devices, current density (*J*)-voltage (*V*)-luminance (*L*), for ITO and graphene electrodes are shown in Fig. 5(a). Regardless of electrode type, OLED devices have similar turn-on voltages (at L = 1cd/m^2) of about 3 V and reach luminance of 1,000 cd/m^2 and 10,000 cd/m^2 at about 4.2 V and 6.1 V, respectively. Nowadays, well synthesized and transferred graphene electrodes exhibit comparable electrical performance to ITO electrodes. As shown in Fig. 5(b), regardless of the presence of a PEDOT:PSS layer, OLED devices show similar electrical characteristics. Such behavior is due to the efficient hole-injection capacity of the HAT-CN layer, which is more or less independent of the work function of the electrode with which it maintains in electrical contact [22–25].

Table 1. External quantum efficiency and CIE color coordinate changes in OLEDs with ITO and graphene electrodes according to the presence of a PEDOT:PSS layer.

	ITO		Graphene	
	w/o PEDOT:PSS	w/ PEDOT:PSS	w/o PEDOT:PSS	w/ PEDOT:PSS
EQE (%)	19.6	19.1	16.6	16.6
Δx[a]	0.052	0.023	0.027	0.010
Δy[a]	0.027	0.059	0.006	0.016
Δxy_{max}[b]	0.054	0.054	0.027	0.018

[a] $\Delta x = x_{max} - x_{min}$, $\Delta y = y_{max} - y_{min}$

[b] $\Delta xy(\theta) = \sqrt{\left(x(\theta) - x(0)\right)^2 + \left(y(\theta) - y(0)\right)^2}$

The external quantum efficiency (EQE) of the OLEDs is summarized in Table 1. ITO-based OLEDs exhibit 15% higher efficiency than graphene-based OLEDs because the absorption of 4-layered graphene induces an inevitable efficiency loss in the devices. It is also noteworthy that a PEDOT:PSS layer does not enhance the efficiency of white OLEDs, in contrast with the case for monochrome OLEDs. ITO and graphene electrodes exhibit similar efficiencies regardless of the presence of a PEDOT:PSS layer. As mentioned previously, a PEDOT:PSS layer can enhance the cavity effect, resulting in high efficiency OLEDs in monochrome emission. However, due to the cavity effect being stronger in these OLED structures, the emission is enhanced at a specific wavelength and its full-width-half-maximum (FWHM) is reduced. Therefore, from the sole perspective of enhancing device efficiency, a PEDOT:PSS layer does not have an advantage in white OLEDs as it is difficult to increase a cavity effect within a fairly wide wavelength region.

Optics EXPRESS

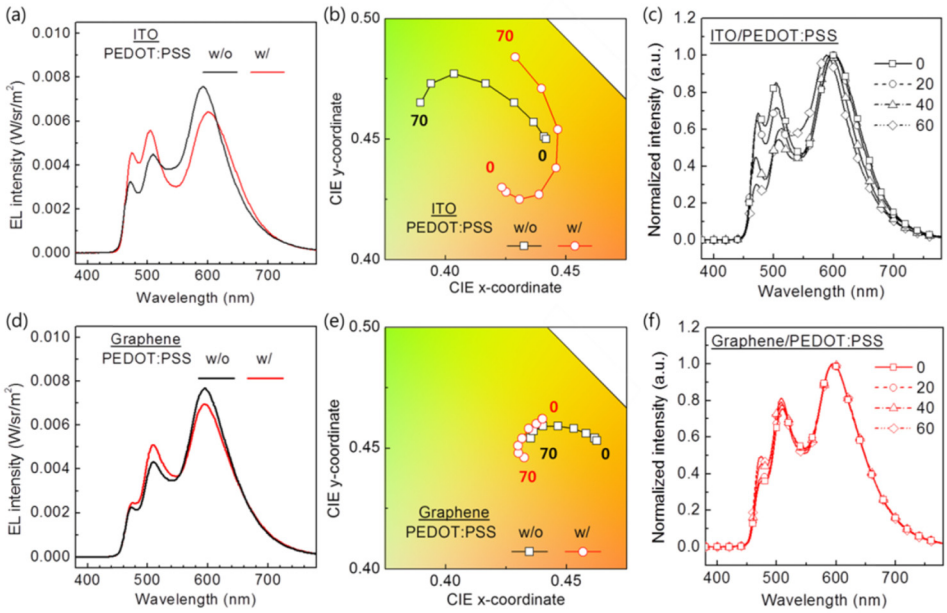

Fig. 6. (a), (d) Electroluminescent intensity at normal direction and (b), (e) CIE color coordinates of OLEDs with ITO and graphene electrodes according to the presence of a PEDOT:PSS layer. Normalized emission spectra for different emission angles of OLEDs based on (c) ITO and (f) graphene, each with a PEDOT:PSS layer.

Figure 6 shows the emission characteristics of white OLEDs with graphene and ITO electrodes. Figures 6(a) and 6(d) show the electroluminescent spectra of OLEDs at a normal direction, with and without PEDOT:PSS, for ITO and graphene, respectively. The change in emission spectra at a normal direction is related to the reflectance of the electrode. The emission of ITO devices dramatically changes when a PEDOT:PSS layer is applied, as the addition of a PEDOT:PSS layer changes not only the intensity but also the phase of the transparent electrode reflectance. As a result, the cavity-enhanced wavelength is shifted to blue and green emission regions, and thus their emission spectrum is increased [21]. Though the reflectance phase is also changed in the graphene-based OLEDs, the spectra change is minimal due to their reflectance being much lower than that of ITO/PEDOT:PSS electrodes, as shown in Fig. 3(a).

For different viewing angles, the changes in the CIE *x*- and *y*-coordinates of ITO and graphene-based devices are displayed in the Figs. 6(b) and 6(e), respectively. The changes in the color coordinates of OLED devices are summarized in Table 1. Similar to the simulation result, the change in the color coordinates of ITO-based OLEDs is 0.054, both with and without the PEDOT:PSS layer. Though graphene alone has a lower reflectance than the other materials, the emission color shift in the graphene/PEDOT:PSS composite-based OLEDs is the lowest. So far, we have only focused on the optical characteristics of transparent electrodes. However, in actual devices, the interference effect originating from a reflective electrode, known as two-beam interference, should be considered [21]. Therefore, the color changes in the graphene-based OLEDs are small but still present. Graphene/PEDOT:PSS composite electrodes generally induce larger color changes than graphene by itself, as shown in the Fig. 4; however, if the OLED structures are well designed, a slightly increased reflectance may compensate for the two-beam interference, resulting in minimal color change in white OLEDs.

Optics EXPRESS

4. Conclusion

In white OLED devices, a strong cavity effect is not desirable, as it results in angular spectral shift and yields insignificant efficiency enhancement. The angular spectral distortion can effectively be removed by adjusting the reflectance of one electrode. To resolve the spectral distortion without sacrificing efficiency, we applied a PEDOT:PSS layer on the anode graphene film. By applying a PEDOT:PSS layer, it was possible to keep the reflectance fairly low (< 2%) within a constant range over a wide range of HTL thicknesses (0-100 nm). Though the graphene-based OLEDs expressed about 15% lower efficiency than ITO-based OLEDs due to the absorption of 4-layered graphene alone, the influence of the PEDOT:PSS layer on OLED efficiency is fairly low. Our graphene/PEDOT:PSS composite-based white OLEDs exhibited 16.6% of EQE, similar to that of graphene-based OLEDs. White OLEDs with graphene/PEDOT:PSS composite electrode demonstrated a much smaller change in CIE color coordinates (0.018) than those based on ITO and ITO/PEDOT:PSS composite electrodes. Moreover, this variance was also lower than that in the OLEDs based on a graphene alone, which has the lowest reflectance of electrode materials. Our optical approach suggests a practical method of stabilizing white-light emission in devices where an interference effect is recognizable.

Funding

Ministry of Trades Industry and Energy/Korea Evaluation Institute of Industrial Technology (MOTIE/KEIT) (10044412).